Journal of Molecular Catalysis B: Enzymatic 68 (2011) 174–180

Contents lists available at ScienceDirect

Journal of Molecular Catalysis B: Enzymatic

journal homepage: www.elsevier.com/locate/molcatb

Mutational analysis of the interaction between a potential inhibitor luteolin and enoyl-ACP reductase (FabI) from *Salmonella enterica*

Jun Min, Xiaoli Zhang, Lei Wang, Xia Zou, Qingye Zhang**, Jin He*

State Key Laboratory of Agricultural Microbiology and National Engineering Research Center of Microbial Pesticides, Huazhong Agricultural University, Wuhan 430070, PR China

ARTICLE INFO

Article history:
Received 1 August 2010
Received in revised form 28 October 2010
Accepted 28 October 2010
Available online 4 November 2010

Keywords:
Enoyl-ACP reductase
FabI
Salmonella enterica
Inhibitor
Luteolin

ABSTRACT

Salmonella enterica is the main cause of food-borne disease worldwide and the emergence of antibiotic-resistant *Salmonella* strains has become a major public health concern. To combat the resistant pathogens, screening of new antibacterials with novel targets or mechanisms of action is very urgent. Luteolin, a traditional Chinese medicine monomer, was proven to be an uncompetitive inhibitor of FabI, the sole enoyl-ACP reductase (ENR) from *S. enterica* (SeFabI), with the inhibition constant (K_i) of 15.1 ± 0.3 μM. Three missense mutations SeFabI[G93V], SeFabI[G93S], and SeFabI[Y156F] were designed to investigate the structure–activity relationship between the inhibitor and the SeFabI target. The specific activities and substrate affinities of SeFabI[G93V] and SeFabI[G93S] were similar to the wild-type SeFabI, while SeFabI[Y156F] lost the substrate catalytic activity, which was consistent with the mechanism for catalytic activity of FabI from *Escherichia coli* (EcFabI) described previously. SeFabI[G93V] mutation showed high level luteolin resistance, which was consistent with the studies in *E. coli* by triclosan. Interestingly, the SeFabI[G93S] showed both luteolin sensitivity and triclosan resistance, and the difference could be explained by the structure discrepancy between luteolin and triclosan. These data imply that the Gly-93 and Tyr-156 are key amino acid residues for luteolin in the active site of the target. As a phytochemical, it has been certified to be safe, thus luteolin would be able to develop as a lead compound for combating resistant bacteria.

1. Introduction

Salmonellosis, caused by the bacteria *Salmonella*, is one of the most common and widely distributed foodborne diseases. Since the beginning of the 1990s, *Salmonella* isolates which are resistant to a range of antimicrobials, including first-choice agents for the treatment of humans, have emerged and are threatening to become a serious public health problem. The resistances result from the use of antimicrobials both in human and animal husbandry. Multi-drug resistances to critically important antimicrobials are compounding the problems. To combat the antibiotic-resistant pathogens, the effective strategy is to identify new antibacterials that function through novel targets or new mechanisms of action [1,2].

Fatty acid synthesis (FAS) pathway is an essential process that supplies precursors for the assembly of important cellular components, including lipopolysaccharides, lipoproteins, phospholipids and the cell envelope. FAS pathways are divided into two distinct forms: FAS-I and FAS-II [3]. Eukaryotes synthesize fatty acid using a multifunctional enzyme complex (FAS-I) [4], while the FAS-II found in prokaryotes consists of individual enzymes that catalyze each step of fatty chain elongation. Subsequently, the obvious differences in the overall architectures between the FAS-I and FAS-II support the proposal that enzymes of FAS-II pathway are selectively targets for the development of novel antibacterials [5].

In particular, the enoyl-ACP reductase (ENR), which catalyzes the last reaction in each round of elongation circle, has become an important target. There are four isoforms, FabI [6], FabK [7], FabL [8] and FabV [9], of ENR among various prokaryotes. For most bacteria, FabI is the unique ENR and shares high overall structural homology, and its variability exists mainly in a mobile loop of amino acids close to the active site (the substrate binding loop) [10]. There are many exciting findings of artificially synthesized inhibitors [6,11–15], including a broad-spectrum antibacterial tri-

Abbreviations: CoA, coenzyme A; DMSO, dimethyl sulfoxide; EcFabI, FabI from *Escherichia coli*; ENR, enoyl-acyl carrier protein reductase; FAS, bacterial fatty acid synthesis; IC_{50}, concentration giving 50% inhibition of activity; IPTG, isopropyl-β-D-thiogalactoside; K_i, inhibition constant; NAD^+, nicotinamide adenine dinucleotide; NADH, nicotinamide adenine dinucleotide reduced form; OE-PCR, overlap extension PCR; PCR, polymerase chain reaction; RMSD, root mean square deviation; SeFabI, FabI from *Salmonella enterica*.

* Corresponding author at: College of Life Science and Technology, Huazhong Agricultural University, No. 1 Sizishan St., Wuhan, Hubei 430070, PR China. Tel.: +86 27 87280670; fax: +86 27 87280670.
** Co-corresponding author.
E-mail addresses: hejin@mail.hzau.edu.cn, hejinhzau@yahoo.com.cn (J. He), qingye_zhang2004@yahoo.com.cn (Q. Zhang).

1381-1177/$ – see front matter © 2010 Elsevier B.V. All rights reserved.
doi:10.1016/j.molcatb.2010.10.007

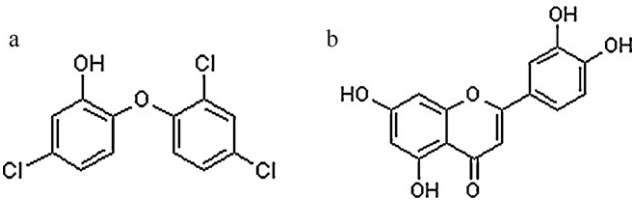

Fig. 1. The structure of (a) triclosan and (b) luteolin.

closan (Fig. 1a) [11,13], which is widely employed in many personal care products, i.e. deodorants, soaps, hand washes and toothpastes. It is a slow, tight-binding inhibitor of FabI, interacting specifically with the enzyme/NAD^+ product complex. However, triclosan is never been used for systemic therapeutic purposes due to its toxicity. Nowadays, numerous investigations have focused on the natural origin FabI inhibitors [16,17], which represent a source of relatively nontoxic. Meanwhile, several detailed kinetic studies coupled with high-resolution crystal structures have provided a solid foundation for the further development of new antibacterials.

In our previous research, the flavonoid luteolin (its structure is shown in Fig. 1b) was proven to be an uncompetitive inhibitor of FabI from *Escherichia coli* (EcFabI) by structure-based virtual screening and experiments [18]. In the present study, mutational analysis of the luteolin-binding region of FabI from *Salmonella enterica* (SeFabI) coupled with cofactor NAD^+ was addressed. The structure–activity studies will lay a solid foundation for further improvement the inhibition activity by structure modification of the phytochemical.

2. Materials and methods

2.1. Materials

Triclosan, crotonyl-CoA, NADH, isopropyl-β-D-thiogalactoside (IPTG) and kanamycin were bought from Sigma–Aldrich. Luteolin with purity 98% up by HPLC method was purchased from Shanghai Tauto Biotech Co., Ltd. (http://www.tautobiotech.com/en/Products_04.htm). His-bind Ni^{2+}-NTA resin was obtained from Invitrogen, while other molecular biology reagents were provided by Takara Biotechnology Co. The purity of all other chemicals was analytical grade.

2.2. Bacterial strains, plasmids and primers

Bacterial strains, plasmids and primers used in this study are listed in Table S1.

2.3. Cloning, expression and purification of SeFabI

The *fabI* gene (GeneID: 6950964) from the *S. enterica* MGSC B090004 was amplified by PCR using the primer pair FabI(F) and FabI(R) (Table S1). The PCR product was digested with *Nde* I and *Hin*d III and cloned into pET-28b(+) at the same restriction sites, so that a His tag was encoded at N-terminus of the coding sequence. The construction sequence was confirmed by DNA sequencing, and the recombinant plasmid pET-*fabI* was then transformed into *E. coli* strain BL21(DE3) competent cells to obtain the SeFabI expression strain BESeI. A single colony of BESeI was used to inoculate into 5 mL of Luria-Bertani (LB) medium containing 30 μg/mL kanamycin, and the culture was grown at 37 °C overnight with shaking. The overnight culture was then inoculated into 500 mL of LB medium containing kanamycin (30 μg/mL) and continuously incubated at 37 °C with vigorous shaking. When the optical density at 600 nm (OD_{600}) reached approximately 1.0, IPTG was added at the final concentration of 1 mM to induce the expression of SeFabI. Subsequently, the culture was shaken at 25 °C for another 16 h. The cells were harvested and resuspended in 30 mL of His binding buffer [20 mM Tris–HCl, 500 mM NaCl, and 10 mM imidazole (pH 7.9)] and lysed by sonication. The cell lysate was removed by centrifugation at 12,000 × *g* for 60 min, and the supernatant was loaded onto a His binding column containing 4 mL of Ni^{2+}-NTA resin. The column was washed with 40 mL of binding buffer, followed by 30 mL of wash buffer [20 mM Tris–HCl, 500 mM NaCl, and 20 mM imidazole (pH 7.9)], and SeFabI was finally eluted by 30 mL of elute buffer [20 mM Tris–HCl, 500 mM NaCl, and 250 mM imidazole (pH 7.9)]. Fractions containing SeFabI were collected, and imidazole was removed by dialysis against 20 mM Tris–HCl (pH 7.5), containing 10% glycerol, 1 mM EDTA, 0.1 mM DTT, and 0.002% Triton X-100. The purity of the enzyme was checked by 12% SDS-PAGE, which gave an apparent molecular mass of ~28 kDa. Protein concentration was assayed by the dye-binding method (Bradford assay) with bovine serum albumin as the standard [19,20].

2.4. PCR-based site-directed mutagenesis

The SeFabI[G93V], SeFabI[G93S], and SeFabI[Y156F] site-directed mutageneses were designed through OE-PCR with the pET-*fabI* as the DNA template [21]. The procedure of the OE-PCR was as follows: (1) in separate PCR reactions, two fragments of *fabI* were amplified by using, for each reaction, one universal [FabI(F) or FabI(R)] and one mutagenic primer [G93V(F) or G93V(R)]. The amplified products were then purified by a gel extraction kit. (2) The resulting DNA fragments were mixed to obtain the full-length reassembled DNA with the mutation site by OE-PCR without primers. (3) The entire DNA was synthesized by PCR with outermost primers and template DNA from step (2). After that, the *fabI* mutations were inserted into pET-28b(+). The sequence of each mutant plasmid was confirmed by DNA sequencing, and the expression and purification of each SeFabI mutant followed the same protocol that was described above for the wild-type SeFabI protein.

2.5. Enzyme assays and kinetic analysis of wild-type and mutant SeFabIs

Various FabI activities were determined by monitoring the oxidation of NADH to NAD^+, which was monitored at 340 nm (ε^{M}_{340} = 6220 M^{-1} cm^{-1}) for 10 min at 30 °C [22]. The standard reaction mixture contained 200 μM crotonyl-CoA, 100 μM NADH, 5 nM enzyme, and luteolin or triclosan in 20 mM Tris–HCl, 150 mM NaCl buffer (pH 7.5) in a total volume of 100 μL. The reaction was initiated by adding the substrate crotonyl-CoA. All the inhibitor compounds were dissolved in DMSO. The concentration of DMSO in all assays was maintained at 5%, which did not significantly affect SeFabI activity according to the control reaction mixture.

The kinetic parameters, K_m (Michaelis constant) and k_{cat} (catalytic constant) of the mutant enzymes for crotonyl-CoA and NADH, were measured for comparison of the specificity constants, k_{cat}/K_m, with that of wild-type SeFabI. The reactions were carried out by changing the concentrations of crotonyl-CoA (50–400 μM) at several fixed concentrations of NADH (50, 100 and 250 μM) or by varying the NADH concentrations (25–250 μM) at several fixed concentrations of crotonyl-CoA (50, 100 and 200 μM). Kinetic parameters were calculated by fitting the data to the Michaelis-Menten equation (Eq. (1)):

$$V = \frac{V_{max}[S]}{K_m + [S]} \quad (1)$$

k_{cat} values were obtained by using the relationship between k_{cat} and V_{max} ($V_{max} = k_{cat}[E]$) [23].

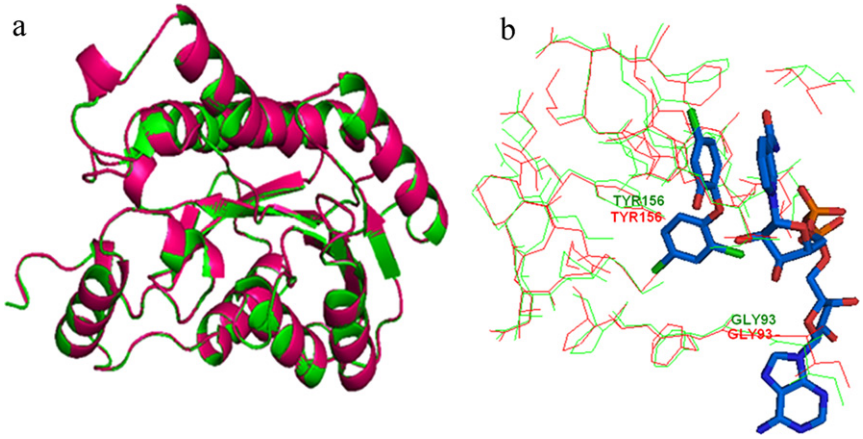

Fig. 2. (a) Schematics for the superposition of 1D8A template and the homology modeling 3D structure of SeFabI. Black ribbon denotes the target protein while grey ribbon is 1D8A template in entire backbone. (b) The active site with triclosan for both template and target SeFabI.

2.6. Determination of IC_{50} values and inhibitor constants (K_i)

The inhibitory activity of the inhibitor compounds was calculated by the following formula:

$$i\% = \left(1 - \frac{v_i}{v_0}\right) \times 100\% \quad (2)$$

$i\%$ is the inhibition rate; v_i is the reaction rate in the present of compound; v_0 is the reaction rate under normal condition.

IC_{50} values of the compounds for SeFabI were determined by plotting the percent inhibition of SeFabI at various concentrations of the compounds. In the standard reaction mixture mentioned above, various concentrations of compounds were added with equal volume of DMSO solvent as an untreated control. The IC_{50} values were determined using at least seven various concentrations, with each concentration assayed in triplicate under saturating substrate conditions. The percent inhibition was calculated from the residual enzymatic activity. The percent inhibition was plotted versus log of the concentrations of the corresponding compounds. The data were analyzed by a nonlinear regression method.

The K_i values of the compounds were determined with respect to crotonyl-CoA. For luteolin, the data were collected against two fixed concentrations of crotonyl-CoA (100 and 150 μM) while varying the luteolin concentrations (4, 8, 12, 16 and 20 μM), and keeping NADH concentration fixed at 100 μM. For positive control, data were collected against two fixed concentrations of crotonyl-CoA (100 and 150 μM) and triclosan concentration was varied from 0.5 nM to 2.5 nM, while NADH concentration was kept at 100 μM. All the data were analyzed by a Dixon plot [24]. Since luteolin was proven to be uncompetitive inhibitor of SeFabI, all the data were analyzed again by Cornish-Bowden plot that was more accurate to calculate the K_i values of uncompetitive inhibitors [25].

2.7. Homology modeling

The interaction mechanism analysis between the active site of target and its ligands is crucial in developing highly potent enzyme inhibitors. Several crystal structures of the ENR [11,26,27] are available from the Protein Data Bank (http://www.rcsb.org/pdb/). With the amino acid sequence of SeFabI from *S. enterica* MGSC B090004 [28], the homology model of SeFabI was built based on sequence alignment. The target sequence was submitted to the SWISS-MODEL sever (Automated Comparative Protein Modeling Sever, Version 3.5, Glaxo Wellcome Experiment Research, Geneva, Switzerland) [29,30] for comparative structure modeling. All hydrogen atoms were subsequently added to the unoccupied valence of heavy atoms at the neutral state using the biopolymer module of SYBYL7.0 program package (http://www.tripos.com). The PROCHECK [31] program was used to check the stereochemical quality of the homology model.

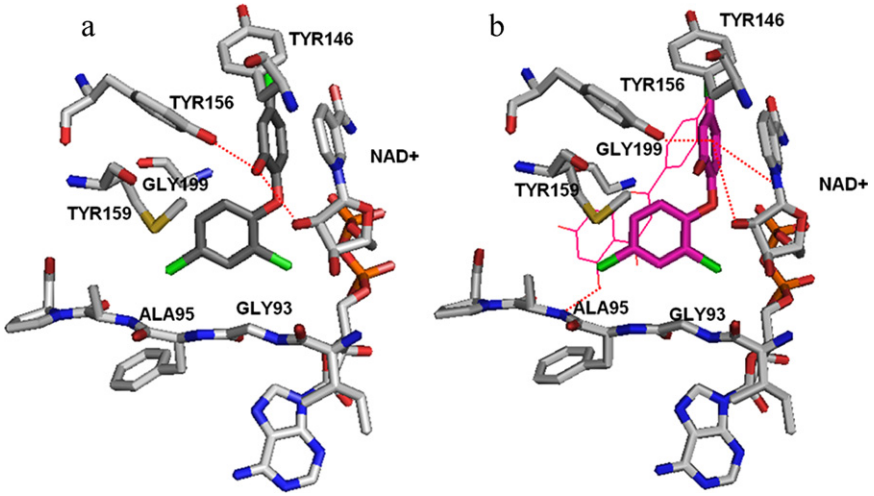

Fig. 3. (a) The binding model of triclosan (black) in the active site of the SeFabI model. The dot-lines represent the hydrogen bonding between the ligand and the amino acid residues. (b) Schematics for the superposition of docking conformation of luteolin (black line) and triclosan (black stick) in the active site of SeFabI homology model.

Table 1
Kinetic parameters for wild-type and mutant SeFabIs.[a]

Enzyme[b]	k_{cat} (min^{-1})	K_m (μM)		k_{cat}/K_m ($\mu M^{-1}\ min^{-1}$)	
		Crotonyl-CoA	NADH	Crotonyl-CoA	NADH
SeFabI	183 ± 5	120 ± 9	45 ± 7	1.5 ± 0.2	4.2 ± 0.8
SeFabI[G93V]	224 ± 8	150 ± 15	52 ± 10	1.5 ± 0.2	4.5 ± 1.0
SeFabI[G93S]	196 ± 7	130 ± 12	40 ± 5	1.5 ± 0.2	5.0 ± 0.8
SeFabI[Y156F]	ND[c]	ND[c]	ND[c]	ND[c]	ND[c]

[a] All kinetic parameters were determined in 20 mM Tris–HCl and 150 mM NaCl at pH 7.5 and 30 °C.
[b] All enzymes contain an N-terminal His tag.
[c] Not determined. Unlike other enzymes, SeFabI[Y156F] had no activity.

2.8. Molecular docking

An accurate three-dimensional (3D) structure of the target enzyme is important for molecular docking and interaction mechanism analyzing. In this study, molecular docking analysis was carried out by the FlexX module of SYBYL package to explore the interaction mechanism between the ligand and target. The docking procedure should be able to correctly predict the binding poses of the inhibitor in the active site. Firstly, the FlexX docking procedure was validated by reproducing the pose of triclosan as shown in its X-ray complex with the target EcFabI (PDB id code: 1D8A). FlexX is a fast automated docking program, which takes ligand's conformational flexibility into account during the docking process by an incremental fragment placing technique [32]. We defined the active site as follows: the structure model of SeFabI and the template protein (1D8A) were superposed at first, and then the triclosan ligand of 1D8A was merged into the corresponding site of the SeFabI model structure. All atoms located within the range of 6.5 Å from any atom of the triclosan ligand in the model were selected into the active site, and the residue was included into the active site if at least one of its atoms was picked out. Other default parameters in the FlexX module were adopted during the FlexX docking. All calculations were performed on a CCNUGrid-based computational environment (CCNUGrid web site: http://202.114.32.71:8090/ccnu/chem/platform.xml).

3. Results and discussion

3.1. Three-dimensional structure model of SeFabI

Up to date, several crystal structures of EcFabI (PDB id codes: 1D8A [11], 1QSG [26], 1C14 [27]) have been reported. 1D8A crystal complex which contains NAD^+ and triclosan (resolution 2.2 Å) was selected as the template to build the 3D structure model of SeFabI. The amino acid sequence identity between the target and the template enzyme was 97.7% (as shown in supporting information Fig. S1). So the homology modeling based on the 1D8A template would allow for a rather straightforward sequence alignment and guarantee the quality of homology modeling. Fig. 2a reveals the superposition of 3D structure from the homology modeling of SeFabI with the 1D8A template, the red ribbon (*black ribbon for grey figure*) is the homology model and the green one (*white one for grey version*) represents the 1D8A template. Just as expected, the overall conformation of the SeFabI model was very similar to the template. And even the amino acids involved in the active site were well conserved between them as displayed in Fig. 2b.

To evaluate the accuracy of the homology model, the obtained structure was checked by PROCHECK for stereo chemical quality. The major amino acid residues of the model were found to occupy the most favored regions of Ramachandran plots, as depicted in Fig. S2, 90.1% of the residues were presented in the most favored regions, 9.0% in the additional regions, 0.9% in the generously allowed regions, and no residue in the disallowed regions, respectively. These signals indicated that the overall conformation of the modeling target enzyme was reliable and reasonable for the following molecular docking analysis.

3.2. Docking analysis

FlexX docking was carried out at first to validate the reliability of the docking procedure adopted herein. Triclosan in crystal structure of 1D8A was selected as a testing molecule. The initial geometric parameters of triclosan backbone was extracted out of 1D8A, added hydrogen atoms and subsequently submitted to a minimization by using the Tripos force field [33], and finally it was docked back into the active site of 1D8A with the FlexX method. All other parameters were selected as default in the FlexX module. The docking result manifested that the binding mode of triclosan obtained by FlexX was almost identical to that of 1D8A crystal complex with root mean square deviation (RMSD) of 0.78 Å (Fig. S3). The docking result illuminated that the FlexX docking procedure is effective to study the FabI system. With the same process and parameters, the known inhibitor triclosan and the potential inhibitor luteolin were docked into the active site of SeFabI to analyze the interaction mechanism between the ligand and SeFabI.

As can be seen in Fig. 3a, the diphenyl ether of triclosan adopted a conformation with a dihedral angle of about 90° between its two phenyl rings. The 2-hydoxy-3-chlorophenyl ring formed a face-to-face stack with the nicotinamide ring of NAD^+, which produced an extensive π–π stacking interactions. The hydrophobic side chains on the protein including Tyr-146 and Tyr-156 formed a pocket and surrounded the nicotinamide and the hydroxychlorophenyl rings. Two hydrogen bonds were observed by the phenolic hydroxyl group (supplies oxygen and hydrogen, separately) of triclosan with the 2′-hydroxyl group of nucleotide ribose and with the phenolic oxygen of Tyr-156. These data are similar to the survey in the crystallographic complex structure of 1D8A with triclosan [11], which promised us that the docking methodology would be effective to predict the binding mode of luteolin to the active site of SeFabI.

The docking mode of luteolin in the active site superposed with triclosan is shown in Fig. 3b. The dihydroxybenzene ring of luteolin displayed a parallel stack with the nicotinamide ring, allowing extensive π–π stacking interactions. Besides the nicotinamide ring, the dihydroxybenzene ring was also surrounded by hydrophobic side chains of Tyr-146 and Tyr-156. The 3′-hydroxyl group of luteolin was involved in three strong hydrogen bonds. Two hydrogen bonds were separately with the 2′-hydroxyl group of the ribose and N1 of the nicotinamide, and the third one was with the phenolic hydroxyl group of Tyr-156. In addition, the 5-hydrogen of luteolin formed a hydrogen bond with Ala-95. The results elucidated that the binding modes of the two ligands with the enzyme/cofactor complex were unusually similar. Therefore, we predicted that luteolin would have the similar inhibition mechanism as triclosan.

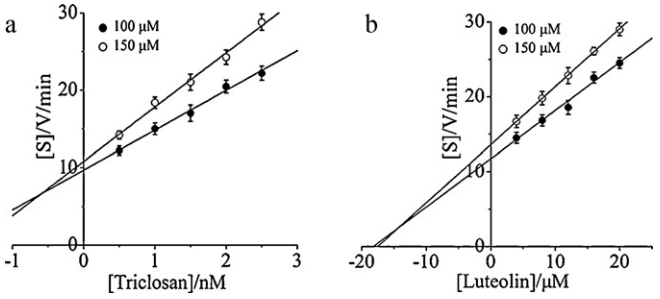

Fig. 4. (a) Cornish-Bowden plot for inhibition kinetics of triclosan for SeFabI with respect to crotonyl-CoA. Triclosan concentration varied in the presence of crotonyl-CoA [100 (●) and 150 μM (○)] with the NADH concentration fixed at 100 μM. The [S]/*V* and [triclosan] concentrations are plotted ([S] = the concentration of crotonyl-CoA). The values are means ± SD of triplicates (SD = standard deviation). (b) Cornish-Bowden plot for inhibition kinetics of luteolin for SeFabI with respect to crotonyl-CoA. Luteolin concentration varied in the presence of crotonyl-CoA [100 (●) and 150 μM (○)] with the NADH concentration fixed at 100 μM. The [S]/*V* and [luteolin] are plotted. The values are means ± SD of triplicates.

3.3. Biological testing of inhibitors

The kinetic parameters, K_m and k_{cat} of the purified SeFabI for crotonyl-CoA and NADH, were measured and summarized in Table 1. The specificity constants of SeFabI, k_{cat}/K_m, for crotonyl-CoA and NADH were 1.5 ± 0.2 and $4.2 \pm 0.8\ \mu M^{-1}\ min^{-1}$, respectively, which coincided well with the values of FabI from *Staphylococcus aureus* [23]. So the obtained SeFabI would be effective enough for the following biological testing.

Triclosan is a slow, reversible, tight-binding inhibitor of FabI, binding preferentially to the FabI/NAD^+ [34]. As a positive control, it was used to certify the accuracy of the experimental method. The K_i value of triclosan was calculated and shown in Fig. 4a, triclosan is obviously an uncompetitive inhibitor of SeFabI with the K_i value of 0.5 ± 0.1 nM, which was consistent with the study of EcFabI [35]. With the same experimental protocol, luteolin was addressed to biological testing. The significant inhibitor with the IC_{50} value of 15.6 ± 0.5 μM was determined, and the inhibition constant (K_i) value was 15.1 ± 0.3 μM, as shown in Fig. 4b. The results suggested that luteolin is an uncompetitive inhibitor of SeFabI, in excellent agreement with the triclosan inhibitor mechanism. So, it was certainly worth further mechanism study.

3.4. Interaction mechanism between luteolin and SeFabIs

In order to recognize the key residues for luteolin binding to the active site, Gly-93 and Tyr-156 were mutated to Val-93, Ser-93 and Phe-156, respectively, according to the binding mode of luteolin to the active site obtained by molecular docking. Previous investigations had demonstrated that mutant proteins of EcFabI[G93V] and EcFabI[G93S] exhibited high level triclosan resistance [35–37], and the resistance mechanism of EcFabI[G93V] was analyzed as well [37]. In the present study, triclosan was docked into the active site of SeFabI model. The Gly-93 was separately substituted by valine and serine to elucidate the triclosan inhibition mechanism. According to Fig. 3a, Gly-93 lies on one side of the active site and the dichlorophenyl ring of triclosan adjoins it. Based on the binding mode and previous study, we could infer that if the Gly-93 was substituted by an amino acid with a bulkier side chain the bioaffinity of triclosan with SeFabI/NAD^+ would decrease tremendously by virtue of the steric clashes. So, mutant enzymes SeFabI[G93V] and SeFabI[G93S] would show high level triclosan resistance. Moreover, SeFabI[G93V] possesses higher resistance than SeFabI[G93S] because the side chain of valine is larger than that of serine (Fig. 5a and b).

Correspondingly, luteolin was docked into the active site of SeFabI[G93V]. As can be noted in Figs. 3b and 6a, the binding mode of luteolin to the active site changed dramatically. The most obvious change was that the 5,7-dihydroxy-4H-chromen-4-one ring and the dihydroxybenzene ring of luteolin exchanged the position with each other. The reason was that the bulkier hydrophobic side chain of valine protruded into the active site and formed the hugeous stereospecific blockade that prevented the binding of 5,7-dihydroxy-4H-chromen-4-one ring to the active site. Consequently, the position exchange could avoid the stereospecific blockade and lead to the decrease of the π–π stacking interaction between the 5,7-dihydroxy-4H-chromen-4-one ring and the nicotinamide. So we predicted that SeFabI[G93V] would show high level luteolin resistance.

In the SeFabI[G93S] case (Fig. 6b), the binding mode of luteolin to the active site of SeFabI[G193S] also changed on account of the steric hindrance of the serine side chain. Compared with the SeFabI[G93V], the serine side chain was smaller and polar, thus the steric hindrance would be much weaker than valine. Especially, the hydroxyl group of serine would form a hydrogen bond with the ketone group of luteolin. Therefore, we could presume that

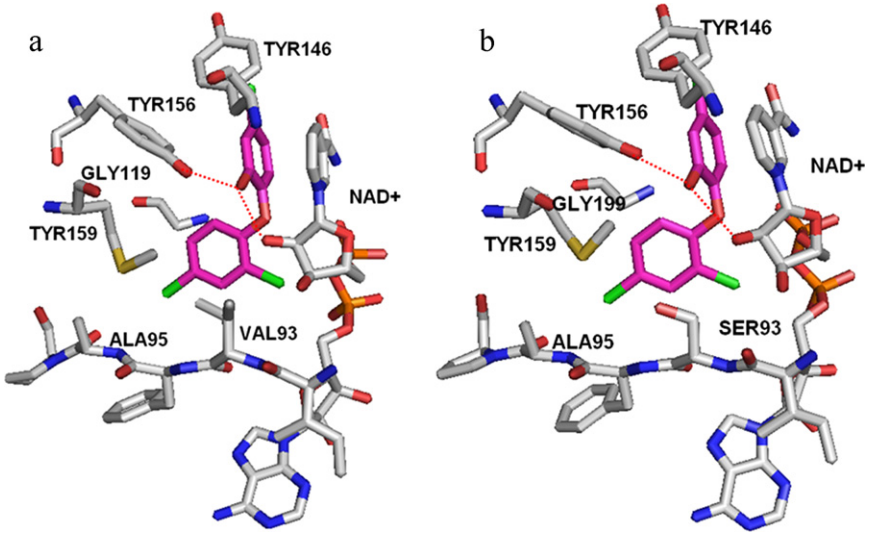

Fig. 5. The binding model of triclosan (black) in the active site of the (a) SeFabI[G93V] model, (b) SeFabI[G93S] model. The dot-lines represent the hydrogen bonding between the ligand and the amino acid residues.

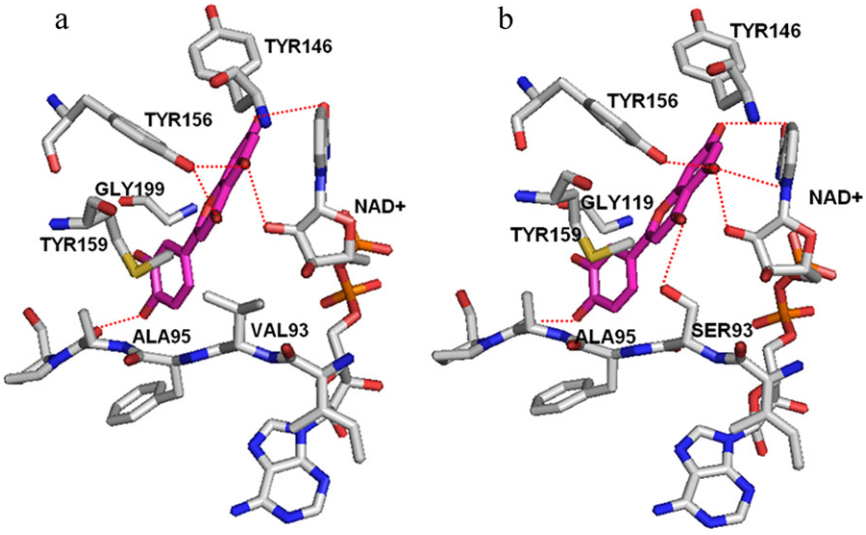

Fig. 6. The binding model of luteolin (black) in the active site of the (a) SeFabI[G93V] model, (b) SeFabI[G93S] model. The dot-lines represent the hydrogen bonding between the ligand and the amino acid residues.

the SeFabI[G93S] would improve the affinity of luteolin than the wild-type SeFabI.

3.5. Kinetic analysis of wild-type and mutant SeFabIs

The kinetic parameters, K_m and k_{cat} of the mutant enzymes for crotonyl-CoA and NADH, were measured for comparison of the specificity constants, k_{cat}/K_m, with that of wild-type SeFabI (Table 1, the enzyme kinetics progress curves were showed in Fig. S4). These data illustrated that SeFabI, SeFabI[G93V] and SeFabI[G93S] had similar specific activities with substrate and cofactor binding characteristics, while the mutant SeFabI[Y156F] dramatically decreased the specific activity and substrate affinity, which was in accordance with the reported catalytic mechanism of EcFabI [38].

The catalytic activities for wild-type and mutant SeFabIs were assayed in the presence of triclosan, and the results were summarized in Table 2. With respect to crotonyl-CoA, triclosan followed uncompetitive inhibitor of SeFabI, SeFabI[G93V] and SeFabI[G93S] with the K_i values of 0.5 ± 0.1, 18.8 ± 0.5 and 2.9 ± 0.2 nM, respectively (Figs. 4a and 7a and b). The inhibition constant for SeFabI was approximately 35- and 5-fold lower than those for SeFabI[G93V] and SeFabI[G93S], respectively. All the experimental results showed no significant difference with the theoretical prediction.

The inhibition of SeFabI[G93V] and SeFabI[G93S] by luteolin was tested to validate the predicted inhibition mechanism. In line with the wild-type SeFabI, just like triclosan, luteolin was testified to be an uncompetitive inhibitor of SeFabI[G93V] and SeFabI[G93S] with the K_i values of 45.4 ± 0.6 and 3.8 ± 0.4 μM, respectively (Fig. 8a and b, Table 2). The K_i of luteolin were approximately 3-fold higher for SeFabI[G93V] and 4-fold lower for SeFabI [G93S], compared with

Table 2
Inhibition constants for triclosan and luteolin binding to wild-type and mutant SeFabIs.

Enzyme	K_i (triclosan) (nM)	K_i (luteolin) (μM)
SeFabI	0.5 ± 0.1	15.1 ± 0.3
SeFabI[G93V] [a]	18.8 ± 0.5	45.4 ± 0.6
SeFabI[G93S] [b]	2.9 ± 0.2	3.8 ± 0.4
SeFabI[Y156]	ND[c]	ND[c]

[a] Triclosan-resistant and luteolin-resistant SeFabI mutant.
[b] Triclosan-resistant but luteolin-sensitive mutant.
[c] Not determined because SeFabI[Y156F] the substrate catalytic activity.

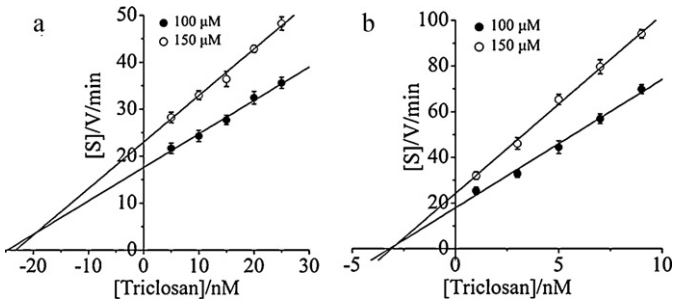

Fig. 7. Cornish-Bowden plot for inhibition kinetics of triclosan for (a) SeFabI[G93V] and (b) SeFabI[G93S] with respect to crotonyl-CoA. Triclosan concentration varied in the presence of crotonyl-CoA [100 (●) and 150 μM (○)] with the NADH concentration fixed at 100 μM. The [S]/*V* and [triclosan] are plotted. The values are means ± SD of triplicates.

that for the wild-type SeFabI. These data indicated that G93V mutation appeared to disturb the binding mode of luteolin to the active site without affecting the substrate catalytic efficiency. The results coincided with our prognosis that the G93V replacement would lead to a dramatic weakening of luteolin binding through the introduction of adverse steric contacts. Therefore, we concluded that the substitution of Gly-93 by an amino acid with a bulkier hydrophobic side chain would lead to the high level luteolin resistance. In contrast to SeFabI [G93V], SeFabI [G93S] showed high level luteolin

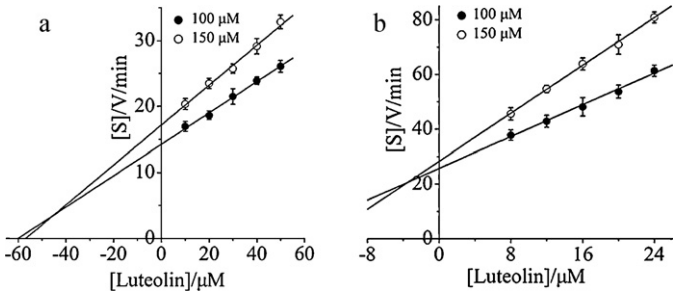

Fig. 8. Cornish-Bowden plot for inhibition kinetics of luteolin for (a) SeFabI[G93V] and (b) SeFabI[G93S] with respect to crotonyl-CoA. Luteolin concentration varied in the presence of crotonyl-CoA [100 (●) and 150 μM (○)] with the NADH concentration fixed at 100 μM. The [S]/*V* and [luteolin] are plotted. The values are means ± SD of triplicates.

sensitivity owing to the hydrogen bond formed between Ser-93 and the ketone group of luteolin. Accordingly, the 93th amino acid was the key site for luteolin binding to the active site of SeFabI.

Through the study, the inhibition mechanism of luteolin for SeFabI was clarified. It should be taken into account that luteolin is extracted from plants and has been used as traditional Chinese medicine for thousands of years, it would be non-toxic and able to develop as a lead compound for some wild-type and resistant bacteria.

4. Conclusions

In present study, luteolin was substantiated to be an uncompetitive inhibitor of SeFabI with the inhibition constant of $15.1 \pm 0.3\ \mu M$. The inhibition mechanism of luteolin was further studied by theoretical simulation analysis with triclosan as a positive control, and then the prognosis was validated through experimental test. Three missense mutations SeFabI[G93V], SeFabI[G93S], SeFabI[Y156F] were designed to investigate the interaction mechanism between luteolin and SeFabI target. The SeFabI[Y156F] mutation significantly lost the substrate catalytic activity, in step with the mechanism provided by Baldock and coworkers, while SeFabI[G93V] and SeFabI[G93S] had little effect on the substrate catalytic activity. SeFabI[G93V] showed high level luteolin resistance, which was consistent with the studies in *E. coli* by triclosan. Interestingly, the SeFabI[G93S] mutation revealed both luteolin sensitivity and triclosan resistance, and the difference could be explained by the structure discrepancy between luteolin and triclosan. These data imply that the Gly-93 and Tyr-156 are key amino acid residues for luteolin in the active site of the target. Furthermore, luteolin was considered to be non-toxic since it exists in many types of plants, including herbs, which had been used as traditional medicine in China for several thousand years. The above findings hold great promise that luteolin or its derivatives have the potency to become antibacterials and deserved further particular study.

Acknowledgements

This work was supported by the Major S&T Projects on the Cultivation of New Varieties of GMO (2009ZX08009-120B) and the Fundamental Research Funds for Central Universities of China (2009PY019). We thank Prof. Wan of Central China Normal University for providing the computer modeling supporting.

Appendix A. Supplementary data

Supplementary data associated with this article can be found, in the online version, at doi:10.1016/j.molcatb.2010.10.007.

References

[1] L. Miesel, J. Greene, T.A. Black, Nat. Rev. Genet. 4 (2003) 442–456.
[2] B.S. Molly, Nat. Rev. Microbiol. 2 (2004) 739–746.
[3] C.O. Rock, J.E. Cronan, Biochim. Biophys. Acta 1302 (1996) 1–16.
[4] S. Smith, A. Witkowski, A.K. Joshi, Prog. Lipid Res. 42 (2003) 289–317.
[5] J.W. Campbell, J.E. Cronan, Annu. Rev. Microbiol. 55 (2001) 305–332.
[6] C. Baldock, J.B. Rafferty, S.E. Sedelnikova, P.J. Baker, A.R. Stuitje, A.R. Slabas, T.R. Hawkes, D.W. Rice, Science 274 (1996) 2107–2110.
[7] R.J. Heath, C.O. Rock, Nature 406 (2000) 145–146.
[8] R.J. Heath, N. Su, C.K. Murphy, C.O. Rock, J. Biol. Chem. 275 (2000) 40128–40133.
[9] R.P. Massengo-Tiasse, J.E. Cronan, J. Biol. Chem. 283 (2008) 1308–1316.
[10] H. Lu, P.J. Tonge, Acc. Chem. Res. 41 (2008) 11–20.
[11] C.W. Levy, A. Roujeinikova, S. Sedelnikova, P.J. Baker, A.R. Stuitje, A.R. Slabas, D.W. Rice, J.B. Rafferty, Nature 398 (1999) 383–384.
[12] C.W. Levy, C. Baldock, A.J. Wallace, S. Sedelnikova, R.C. Viner, J.M. Clough, A.R. Stuitje, A.R. Slabas, D.W. Rice, J.B. Rafferty, J. Mol. Biol. 309 (2001) 171–180.
[13] S.L. Parikh, G. Xiao, P.J. Tonge, Biochemistry 39 (2000) 7645–7650.
[14] W.H. Miller, M.A.K.A. Seefeld, I.N. Uzinskas, W.J. Burgess, D.A. Heerding, C.C. Yuan, M.S. Head, D.J. Payne, S.F. Rittenhouse, T.D. Moore, S.C. Pearson, V. Berry, W.E. DeWolf Jr., P.M. Keller, B.J. Polizzi, X. Qiu, C.A. Janson, W.F. Huffman, J. Med. Chem. 45 (2002) 3246–3256.
[15] X. He, A. Alian, R. Stroud, P.R. Ortiz de Montellano, J. Med. Chem. 49 (2006) 6308–6323.
[16] T. Banerjee, S.K. Sharma, N. Surolia, A. Surolia, Biochem. Biophys. Res. Commun. 377 (2008) 1238–1242.
[17] C.J. Zheng, M.J. Sohn, W.G. Kim, J. Antimicrob. Chemother. 63 (2009) 949–953.
[18] J.J. Yao, Q.Y. Zhang, J. Min, J. He, Z.N. Yu, Bioorg. Med. Chem. Lett. 20 (2010) 56–59.
[19] Y. Yu, T. Asuka, Y. Nana, E. Khalil, Y. Eitora, M. Hanae, F. Noboru, S. Keiji, S. Yoshihiro, Y. Toshiharu, J. Mol. Catal. B: Enzym. 67 (2010) 104–110.
[20] M.M. Bradford, Anal. Biochem. 72 (1976) 248–254.
[21] Y.F. An, J.F. Ji, W.F. Wu, A.G. Lv, R.B. Huang, Y.T. Wei, Appl. Microbiol. Biotechnol. 68 (2005) 774–778.
[22] M. Kapoor, C.C. Reddy, M.V. Krishnasastry, N. Surolia, A. Surolia, Biochem. J. 381 (2004) 719–724.
[23] H. Xu, T.J. Sullivan, J. Sekiguchi, T. Kirikae, I. Ojima, C.F. Stratton, W.M. Mao, F.L. Rock, M.R.K. Alley, F. Johnson, S.G. Walker, P.J. Tonge, Biochemistry 47 (2008) 4228–4236.
[24] K. Nazari, A. Mahmoudi, M. Khosraneh, Z. Haghighian, A.A. Moosavi-Movahedi, J. Mol. Catal. B: Enzym. 56 (2009) 61–69.
[25] A. Cornish-Bowden, Biochem. J. 137 (1974) 143–144.
[26] M.J. Stewart, S. Parikh, G. Xiao, P.J. Tonge, C. Kisker, J. Mol. Biol. 290 (1999) 859–865.
[27] X. Qiu, C.A. Janson, R.I. Court, M.G. Smyth, D.J. Payne, S.S. Abdel-Meguid, Protein Sci. 8 (1999) 2529–2532.
[28] N.R. Thomson, D.J. Clayton, D. Windhorst, G. Vernikos, S. Davidson, C. Churcher, M.A. Quail, M. Stevens, M.A. Jones, M. Watson, A. Barron, A. Layton, D. Pickard, R.A. Kingsley, A. Bignell, L. Clark, B. Harris, D. Ormond, Z. Abdellah, K. Brooks, I. Cherevach, T. Chillingworth, J. Woodward, H. Norberczak, A. Lord, C. Arrowsmith, K. Jagels, S. Moule, K. Mungall, M. Sanders, S. Whitehead, J.A. Chabalgoity, D. Maskell, T. Humphrey, M. Roberts, P.A. Barrow, G. Dougan, J. Parkhill, Genome Res. 18 (2008) 1624–1637.
[29] S.H. Kim, S.P.Y.J. Yoo, J. Mol. Catal. B: Enzym. 55 (2008) 130–136.
[30] T. Schwede, J. Kopp, N. Guex, M.C. Peitsch, Nucleic Acids Res. 31 (2003) 3381–3385.
[31] T.K. Prachumporn, R. Khakhanang, C. Khuanjarat, T. Nusra, S. Penporn, P. Chompoonuth, O. Amornrat, S. Jisnuson, J. Mol. Catal. B: Enzym. 67 (2010) 257–265.
[32] B. Kramer, M. Rarey, T. Lengauer, Proteins: Struct. Funct. Genet. 37 (1999) 228–234.
[33] M. Clark, R.D. Cramer III, N. Van Opdenbosch, J. Comput. Chem. 10 (1989) 982–1012.
[34] W.H. Ward, G.A. Holdgate, S. Rowsell, E.G. McLean, R.A. Pauptit, E. Clayton, W.W. Nichols, J.G. Colls, C.A. Minshull, D.A. Jude, A. Mistry, D. Timms, R. Camble, N.J. Hales, C.J. Britton, I.W. Taylor, Biochemistry 38 (1999) 12514–12525.
[35] S. Sivaraman, J. Zwahlen, A.F. Bell, L. Hedstrom, P.J. Tonge, Biochemistry 42 (2003) 4406–4413.
[36] R.J. Heath, Y.T. Yu, M.A. Shapiro, E. Olson, C.O. Rock, J. Biol. Chem. 273 (1998) 30316–30320.
[37] R.J. Heath, J.R. Rubin, D.R. Holland, E. Zhang, M.E. Snow, C.O. Rock, J. Biol. Chem. 274 (1999) 11110–11114.
[38] C. Baldock, J.B. Rafferty, A.R. Stuitje, A.R. Slabas, D.W. Rice, J. Mol. Biol. 284 (1998) 1529–1546.